

Abstract

Contents

1	Introduction	5
1.1	Living with fluids	5
1.2	Outline of the thesis	5
2	Introduction	6
2.1	Overview	6
2.2	Transitional wall-bound shear flows	8
2.2.1	Linear Stability Analysis	10
2.2.2	Nonlinear dynamical systems	13
2.2.3	Spatiotemporal transitional flows	14
2.3	Rayleigh-Bénard convection (RBC)	17
2.4	Rayleigh-Bénard Poiseuille (RBP) flows	20
2.4.1	Thesis Outline	20
3	Numerical Techniques	19
3.1	Method of weighted residuals	19
3.2	The Spectral/hp element methods	22
3.3	Temporal Discretisation	24
3.4	Velocity correction scheme for incompressible Navier Stokes equations	26
3.5	Linear Stability Analysis	28
3.6	Edge Tracking	28
4	Transitional Rayleigh-Bénard Poiseuille flows	29
4.1	Introduction	29
4.1.1	Rayleigh-Bénard Poiseuille (RBP) flows	29
4.1.2	Rayleigh-Bénard convection (RBC)	30
4.1.3	Plane Poiseuille flows (PPF)	30
4.1.4	Objectives and organisation	31
4.2	Problem formulation	31
4.2.1	Governing equations	31
4.2.2	Numerical Methods	32
4.2.3	<i>Ra-Re</i> sweep	33
4.2.4	Linear Stability Analysis	33
4.3	<i>Ra-Re</i> Phase Space	34
4.3.1	Classification	34
4.3.2	Spatiotemporal intermittent rolls	36

4.3.3	Coexistence with turbulent bands	38
4.4	The role of longitudinal rolls	39
4.4.1	The thermally-assisted sustaining process (TASP) in a confined domain	39
4.4.2	Variation of Ra and Re on the thermally sustained turbulent process within $\Gamma = \pi/2$	47
4.4.3	Extending to large domains, $\Gamma = 4\pi$	53
4.5	Conclusions	53
5	The state space structure of Spiral Defect Chaos	55
5.1	Introduction	55
5.1.1	Multiple convection states	55
5.1.2	Spiral defect chaos	56
5.1.3	Scope of this study	56
5.2	Problem formulation	57
5.2.1	Rayleigh-Bénard convection (RBC)	57
5.2.2	Numerical method	58
5.2.3	Linear stability analysis of ISRs	58
5.3	Transient SDC and elementary states in minimal domain	59
5.4	Multiplicity of edge states	65
5.5	Unstable ideal straight rolls	69
5.5.1	Pathways leading to ISRs - heteroclinic orbits	73
5.5.2	Pathways leading to elementary states	76
5.5.3	A pathway to SDC in an extended domain $\Gamma = 4\pi$	78
5.6	Concluding remarks	82
6	Conclusions	84
A	Appendices	85
A.1	Non-dimensionalisation	85
A.2	Governing equations for Rayleigh-Bénard convection	86
A.3	Simulation parameters for Ra - Re sweep	86
A.4	First- and second-order statistics of the buoyancy- and shear-driven regime	86
A.4.1	Buoyancy-driven regime	86
A.4.2	Shear-driven regime	89
A.5	Growth rates of primary instabilities	89
A.6	Verification of linear stability analysis	92
A.7	Other elementary states and ISRs	92

Chapter 2

Introduction

2.1 Overview

A broad class of fluid motions driven by buoyancy and frictional forces are found in the study of thermal convective and wall-bounded shear flows. Their combined effects leading to rich behaviour, spanning across wide interests in engineering and meteorology applications. In small length scales of $L \sim 1\text{cm}$, this concerns the cooling of silicon chips, where the fluid experiences shear from the walls, and buoyancy from heating. One of the main innovations in this field is on the exponential increase in computing power in the 20th century, by squeezing more transistors into a single silicon chip. Moore's law predicts that the amount of transistors on a single chip will double every two years. One of the major limitations is on dissipating the excessive heat from the silicon chip. In many cases, a fluid (air/water/refrigerant) act as a medium, transporting heat away from the components preventing overheating [Kennedy and Zebib, 1983, Ray and Srinivasan, 1992]. In moderate length scales, $L \sim 1\text{m}$, the interaction between buoyancy and frictional forces concern the fabrication of uniform thin films in chemical vapour deposition (CVD) [Evans and Greif, 1991, Jensen et al., 1991]. The CVD process usually involves a reactive gases, carried by inert gases convected through a channel which has a heated substrate. Upon heating, the reactant gases react chemically at substrate, depositing a material where thin films are fabricated, such as silicon layers. In many cases, the important qualities of the CVD process is in the uniformity of thin film, and the sharpness between their interfaces. Interactions between shear and buoyancy forces often lead to development of a boundary layer and thermoconvective rolls, impacting the homogeneity of deposition, posing a challenge for a uniform layer of film. In the largest of scales, $L \sim 1\text{km}$, parallel bands of cumulus clouds over the Norwegian Sea, known as clouds streets, extending for several hundreds of kilometres. These cloud streets develop when the relative warmer Norwegian sea heats up the colder air blowing from the North [nor]. The heated air (or thermals) rises towards the atmosphere while transporting water vapour, condenses into visible clouds. The cooler air falls towards the sea, forming the distinct parallel cylinders of rotating air known as thermconvective rolls.

The common denominator of the examples given above is in the interaction between shear and buoyancy forces driven fluid motion, the main focus of this thesis. We note that by restricting our analysis to two forces, other physical mechanisms such as phase change, chemically reactions and latent heat of evaporation are neglected, which could be important in the cooling of electronic components, CVD, and atmospheric boundary layers respectively [Vallis et al., 2019]. We consider an idealised setup, without any geometric complexity, referred to as the Rayleigh-Bénard-Poiseuille

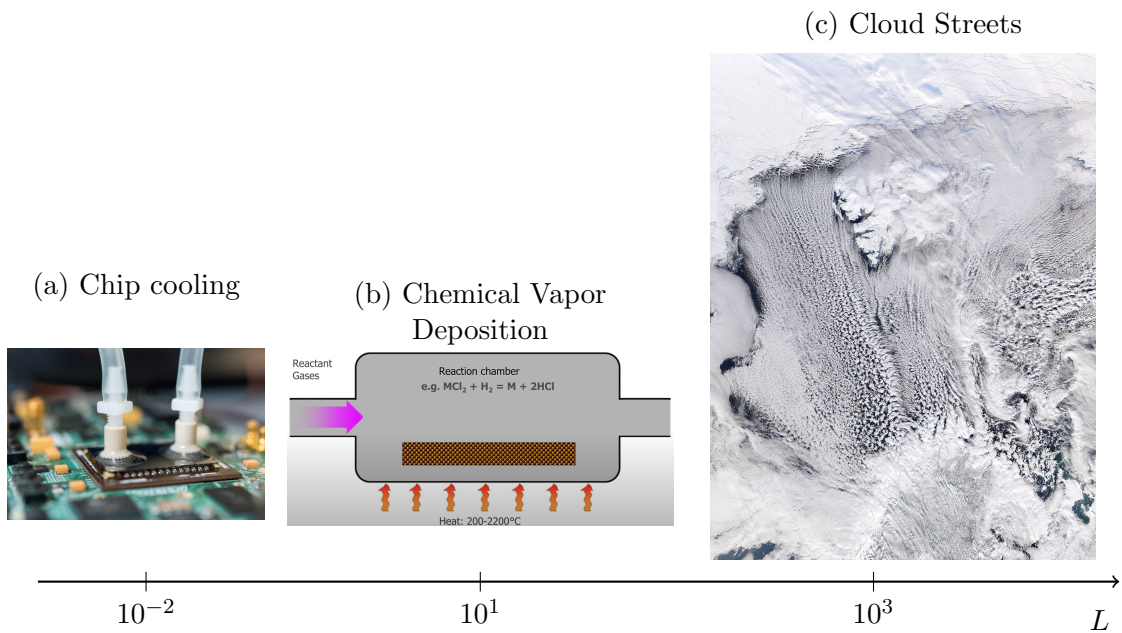


Figure 2.1: Fluid flow due to shear and buoyancy forces across length scales, $L \in [1\text{cm}, 1\text{km}]$, such as (a) chip cooling, (b) chemical vapour deposition and (c) formation of cloud streets.

(RBP) flow. RBP flows describe the motion of a fluid between two infinitely extended parallel walls, heated from below and cooled from the top, driven by a pressure gradient. The RBP system combines the two paradigmatic flow configurations; the classical Rayleigh-Bénard convection (RBC) and the plane Poiseuille flow (PPF), driven by buoyancy and shear forces, respectively. The onset of convection and the transition to subcritical shear-driven turbulence has been well studied independently over the past decades, however, the transitional regime where both forces interact remains largely unexplored. Understanding the transition to turbulence in this regime can have implications for applications across a range of scales mentioned previously.

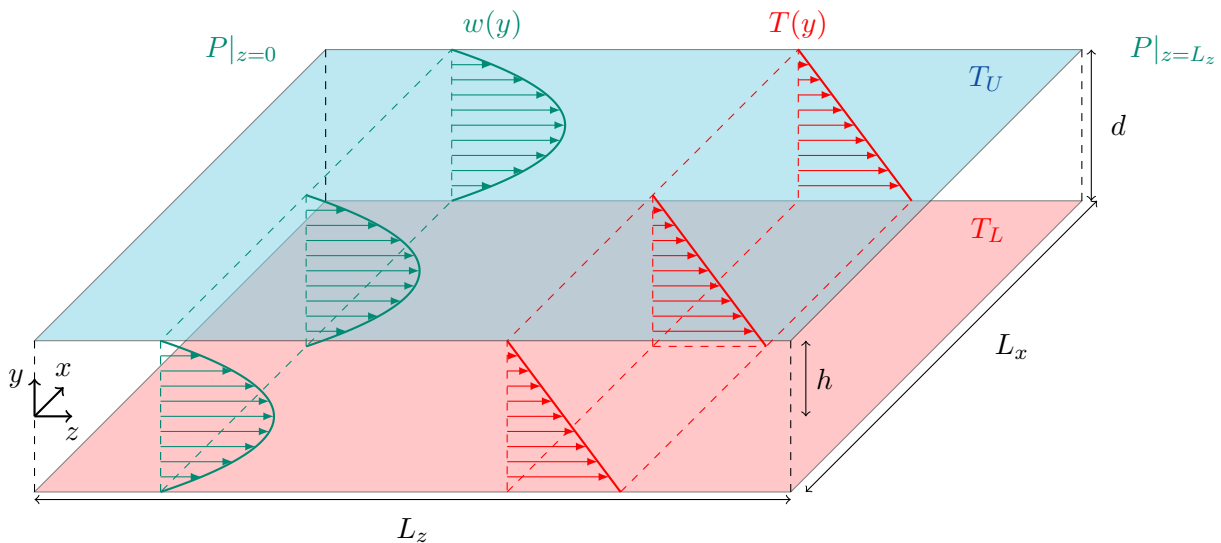


Figure 2.2: The Rayleigh-Bénard Poiseuille (RBP) flow configuration.

The RBP configuration is illustrated in figure 2.1, where $z^*, y^*, x^*, L_z, L_x, d, h$ refer to the streamwise, spanwise, wall-normal coordinates, length, span, depth and half-height of the domain respectively.

tively. We note that the asterisks*, refer to variables in dimensional form. The flow is driven by a pressure gradient along the streamwise z^* direction, $\Delta P^* = P^*|_{z^*=0} - P^*|_{z^*=L_z} < 0$, leading to the formation of a laminar Poiseuille flow, $w^*(y^*)$, for a sufficiently small ΔP . In this study, we will only consider fully-developed flow, where the boundary layer from the top and the bottom wall meets at the midplane, $y^* = 0$, and entrance effects are neglected. The RBP configuration is also unstably stratified, such that the temperature difference between the lower, T_L , and upper wall, T_U , is always positive, $\Delta T = T_L - T_U > 0$, leading to a stable linear conduction profile along the wall-normal direction, $T(y^*)$, if ΔT is kept sufficiently small.

In the absence of a pressure gradient, the RBP configuration reduces to the classical Rayleigh-Bénard convection problem, bringing about buoyancy-driven convection for a sufficiently large unstable stratification. In the limiting case without unstable stratification, $\Delta T = 0$, the system reduces to the wall-bounded plane Poiseuille flow (PPF), where the transition towards subcritical shear-driven turbulence may be expected for a sufficiently large pressure gradient.

For instance, do buoyancy forces promote the transition to shear-driven turbulence and how does shear influence the convection? To describe the motion of the fluid in RBP configurations, we consider non-dimensionalised Navier-Stokes equations with Boussinesq approximations,

$$\frac{\partial \mathbf{u}}{\partial t} + (\mathbf{u} \cdot \nabla) \mathbf{u} = -\nabla p + \frac{1}{Re} \nabla^2 \mathbf{u} + \frac{Ra}{Re^2 Pr} \theta, \quad (2.1a)$$

$$\frac{\partial \theta}{\partial t} + (\mathbf{u} \cdot \nabla) \theta = \frac{1}{Re Pr} \nabla^2 \theta, \quad (2.1b)$$

$$\nabla \cdot \mathbf{u} = 0. \quad (2.1c)$$

where $\mathbf{u}(\mathbf{x})$, $\theta(\mathbf{x})$, $p(\mathbf{x})$ refers to the nondimensionalised velocity, temperature and pressure respectively. The key control parameters for RBP flows are the Rayleigh number, Ra , Reynolds number, Re , Prandtl number Pr , which are defined as follows,

$$Ra = \eta g d^3 \Delta T / \nu \kappa, \quad Re = W_c h / \nu, \quad Pr = \kappa / \nu, \quad \Gamma = L / 2d, \quad (2.2)$$

where η , g , ΔT , ν , κ , W_c , h , d , L are the thermal expansion coefficient, acceleration due to gravity, temperature difference between the bottom and top wall, kinematic viscosity, thermal diffusivity, laminar centreline velocity, domain's half-depth, full-depth, length or span respectively.

We describe important historical of hydrodynamic stability of planar shear flows and their theoretical frameworks in §2.2. Theoretical frameworks used in the study of stability of flow such as linear stability, nonlinear dynamical systems and spatiotemporal character of transitional shear flows will be outlined. This followed the historical developments of Rayleigh-Bénard convection (RBC), where concepts of the stability of fluid flows will be utilised in §2.3. After which, we describe the historical developments of RBP flows §2.4, and the outline of the thesis will be give in §2.4.1.

2.2 Transitional wall-bound shear flows

Wall-bounded shear flows concerns the motion of a fluid travelling in parallel to solid surfaces, referred to as walls. To satisfy the no-slip boundary condition at the wall, the fluid closest to the wall comes to a rest, generating a regular velocity gradient in the direction perpendicular away from the wall.

In Newtonian fluids, shear stresses are directly proportionate to the velocity gradient by the fluids kinetic viscosity, ν , given as,

$$\tau = \nu \frac{\partial u}{\partial y}, \quad (2.3)$$

where τ , ν , and $\frac{\partial u}{\partial y}$ refers to shear, kinematic viscosity and velocity gradients. Examples flows include the pressure-driven plane Poiseuille flow (PPF), pipe (Hagen-Poiseuille) flow, plane Couette flow and flat plate boundary layers. These geometrically simple examples enables a convenient framework amenable to the mathematical analysis of fluid motion under shear. A central question in this field is predicting the transition to turbulence, specifically, at what point does turbulence emerge as shear increases?

The earliest investigation into this transition dates back to the pipe flow experiments of [Reynolds \[1883\]](#). In his experimental setup, the flow speed through the pipe could be controlled by regulating the inlet pressure, while injecting dye to visualise the flow, as illustrated in figure 2.3(a). At low speeds, the fluid remained laminar, whereby the fluid layers moved in smooth parallel ‘laminates’, resulting to a single streak of steady dye in figure 2.3(b). As the speed increased, the dye begin to exhibit irregular ‘sinuous’ motions interspersed with laminar regions shown in figure 2.3(c). This is now referred to as the transitional/intermittent regime, alternating between the laminar and turbulent states. Beyond a critical speed, the dye breaks down entirely into chaotic ‘eddies’, mixing with the surrounding fluid and discolouring the flow with dye downstream in figure 2.3(d). This regime is now identified as turbulence. Reynolds conjectured that the threshold between the laminar, transitional and turbulent regimes could be characterised by non-dimenisonal parameter, now known as the Reynolds number, $Re = UD/\nu$, where U is the centerline velocity in the pipe, D , the pipe diameter and ν , the kinematic viscosity. He observed that flow through the pipe remained ‘stable’ and laminar for $Re < 1900$, while it became ‘unstable’ and turbulent for $Re > 2000$ [[Reynolds, 1895](#)]. His remarks led to the concept of the stability of fluid flows.

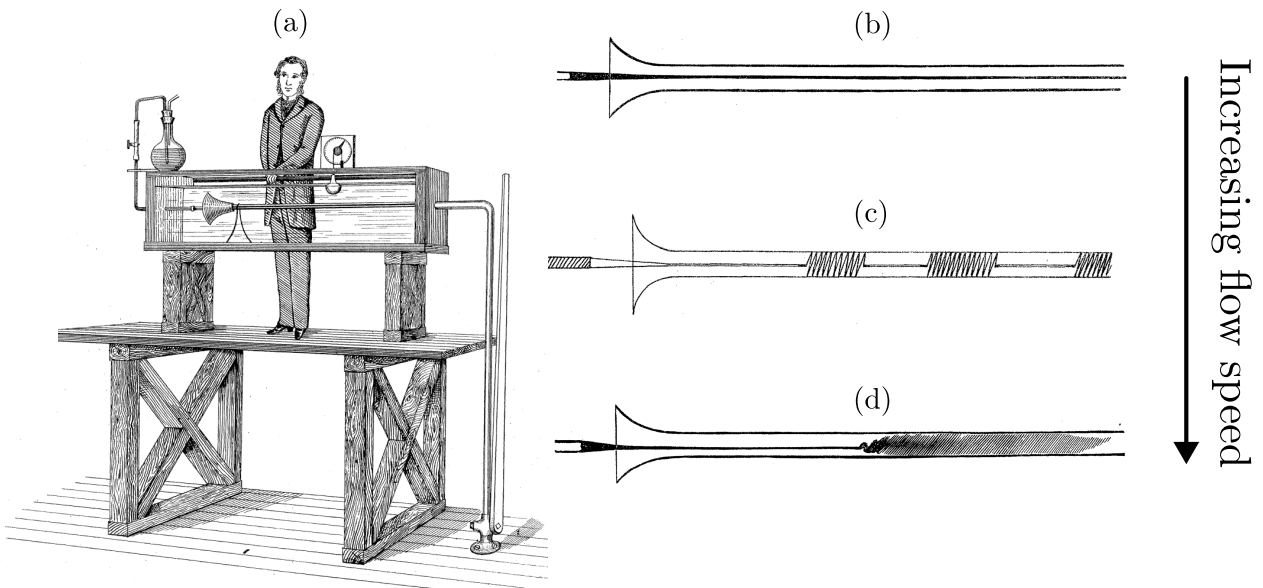


Figure 2.3: (a) Osbourne Reynolds pipe experiment with the dye injection apparatus, illustrating the (b) laminar flow, (c) intermittent regime and (d) turbulent flow as the flow speed is increased, taken from [[Reynolds, 1883](#)].

2.2.1 Linear Stability Analysis

Following Reynolds' experiment, interest towards the mathematical analysis of the stability of fluid flows grew in early 20st century. The typical approach begins with decomposing the velocity field, $\mathbf{u}(\mathbf{x}, t)$, into a laminar (base) state, $U(y)$ (assumed to depend only on the wall-normal direction here), and the velocity perturbations, $\mathbf{u}'(\mathbf{x}, t)$, with pressure similarly decomposed as,

$$\mathbf{u}(\mathbf{x}) = U(y) + \mathbf{u}'(\mathbf{x}, t), \quad \text{and} \quad p(\mathbf{x}, t) = P(x) + p'(\mathbf{x}, t). \quad (2.4)$$

Next, we substitute the formulations for the decomposed velocity and pressure into the Navier-Stokes equations of equation (2.1) and drop the nonlinear perturbations terms $(\mathbf{u}' \cdot \nabla)\mathbf{u}'$,

$$\frac{\partial \mathbf{u}'}{\partial t} + (U \cdot \nabla)\mathbf{u}' + (\mathbf{u}' \cdot \nabla)U = -\nabla p' + \frac{1}{Re}\nabla^2\mathbf{u}', \quad (2.5a)$$

$$\nabla \cdot \mathbf{u}' = 0, \quad (2.5b)$$

resulting to the linearised Navier-Stokes equations. This commonly followed by introducing a wavelike ansatz (mode) defined by streamwise and spanwise wavenumbers, α, β and complex frequency, ω . In general two ways to analyse the linearised Navier-Stokes equations by considering the behaviour of each mode independently in §2.2.1 and their coupled dynamics in §2.2.1

Modal analysis

It is convenient to eliminate the pressure terms by transforming equation (2.5) using the wall-normal perturbation velocity, v' , and wall-normal vorticity, $\eta' = \partial u'/\partial z - \partial w'/\partial x$, variables. Using (v, η) , introduce an ansatz (mode) for them,

$$v'(\mathbf{x}, t) = \tilde{v}(y)e^{i(\alpha x + \beta z - \omega t)}, \quad \text{and} \quad \eta'(\mathbf{x}, t) = \tilde{\eta}(y)e^{i(\alpha x + \beta z - \omega t)}. \quad (2.6)$$

where α, β, ω denotes the streamwise and spanwise wavenumbers, and complex frequency (i.e. $\omega = \omega_r + i\omega_i$), respectively. Next, we substitute the ansatz into equation 2.5, leading to the classical Orr-Sommerfeld and Squire equations [Orr, 1907, Sommerfeld, 1909, Squire, 1933, Schmid and Henningson, 2001],

$$\begin{bmatrix} -i\omega \begin{pmatrix} k^2 - \mathcal{D}^2 & 0 \\ 0 & 1 \end{pmatrix} + \begin{pmatrix} \mathcal{L}_{OS} & 0 \\ i\beta U' & \mathcal{L}_{SQ} \end{pmatrix} \end{bmatrix} \begin{pmatrix} \tilde{v} \\ \tilde{\eta} \end{pmatrix} = \mathbf{0}, \quad (2.7)$$

where \mathcal{L}_{OS} and \mathcal{L}_{SQ} refers to the Orr-Sommerfeld and Squire operators given as,

$$\mathcal{L}_{OS} = i\alpha U(k^2 - \mathcal{D}^2) + i\alpha U'' + \frac{1}{Re}(k^2 - \mathcal{D}^2)^2, \quad (2.8a)$$

$$\mathcal{L}_{SQ} = i\alpha U + \frac{1}{Re}(k^2 - \mathcal{D}^2). \quad (2.8b)$$

$k^2, \mathcal{D}, U', U''$ denotes the sum of squared wavenumbers, $k^2 = \alpha^2 + \beta^2$, differential operator in y , first- and second- derivative of the laminar velocity, respectively. Equation (2.7) is simply an eigenvalue problem which could be represented as,

$$\mathbf{L}\tilde{\mathbf{q}} = i\omega\mathbf{M}\tilde{\mathbf{q}} \quad (2.9)$$

where,

$$\mathbf{L} = \begin{pmatrix} \mathbf{L}_{OS} & 0 \\ i\beta U' & \mathcal{L}_{SQ} \end{pmatrix}, \quad \mathbf{M} = \begin{pmatrix} k^2 - \mathcal{D}^2 & 0 \\ 0 & 1 \end{pmatrix}, \quad \tilde{\mathbf{q}} = \begin{pmatrix} \tilde{v} \\ \tilde{\eta} \end{pmatrix}. \quad (2.10)$$

and $i\omega$ refers to the eigenvalue. The aim of linear stability analysis is to determine the critical Reynolds number, Re_c , which is defined as the lowest value of Re over α and β , such that $Im[\omega] = 0$. For $Re > Re_c$, perturbations could grow exponentially, departing from the laminar state. In other words, we consider the behaviour of each $\alpha - \beta$ mode independently, herein referred to as *modal* analysis. Squire's theorem implies that for any unstable three-dimensional perturbations, $\beta \neq 0$, there exist an unstable two-dimensional perturbation, $\beta = 0$ with a lower Re_c [Squire, 1933]. Therefore, the unstable perturbations of wall-bounded shear flows at Re_c must be two-dimensional. The theoretical calculations was first perform by Tollmien [1928] and Schlichting [1933] for a flat-plate boundary layer flow, yielding a critical Reynolds number based on streamwise distance x of $Re_{x,c} = Ux_c/\nu = 520$ [Schlichting and Gersten, 2017]. In their honour, the unstable two-dimensional perturbations of the Orr-Sommerfeld operator is referred to as Tollmien-Schlichting (T.S) waves. For plane Poiseuille flow [Orszag, 1971] with a critical wavenumber of $\alpha_c = 1.02$. However, turbulence in plane Poiseuille flows have been observed at much lower Reynolds number, $Re \sim 1000 - 2000$, contradicting the results from linear stability analysis. Likewise, the onset of turbulence appear near $Re_{x,c} \approx 5 \times 10^5$ for flat plat boundary layer. A similar result holds for the plane Couette flow [Meseguer and Trefethen, 2003]. Despite its limitation, linear analysis analysis succeeds in predicting the critical Rayleigh number in Rayleigh-Bénard convection.

Non-modal stability

One of a major limitation of linear stability analysis considered above is that it treats each eigenmode independently, referred to as *modal* analysis. However, the interaction between decaying eigenmodes may lead to a short-term amplification of perturbations, before eventually decaying. This phenonemon is referred to as *transient growth*, and the method of analysis is referred to as *non-modal* analysis, related to the normality of the linear Orr-Sommerfeld operator [Schmid, 2007]. To demonstrate an

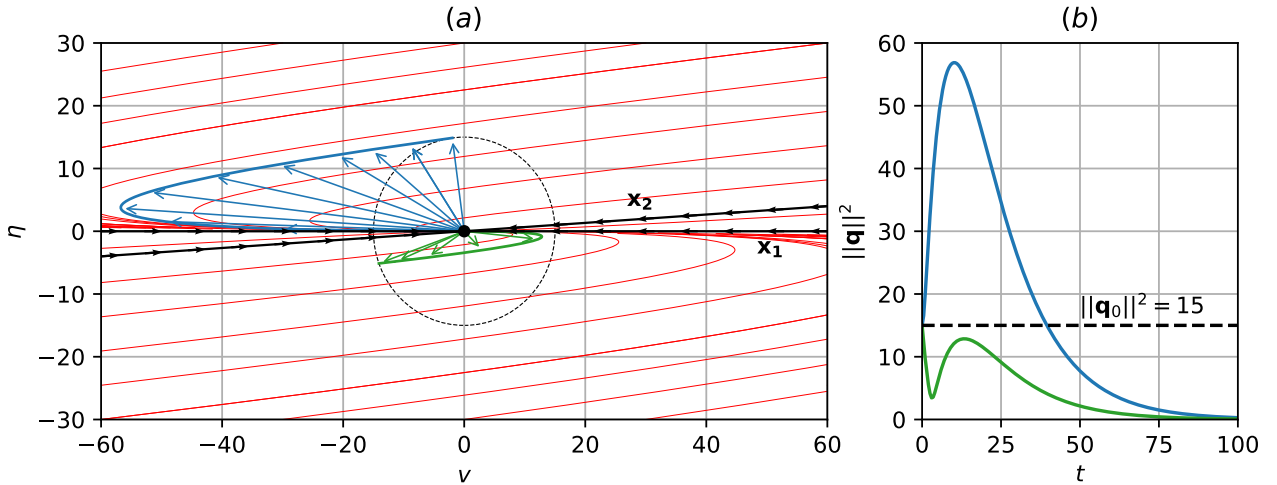


Figure 2.4: (a) The phase portrait of the toy model with $Re = 15$, (b) Transient growth.

example of transient growth, we consider a two-dimensional toy model governing the time-evolution

of \mathbf{q} ,

$$\frac{d}{dt} \begin{pmatrix} v \\ \eta \end{pmatrix} = \begin{pmatrix} -\frac{1}{Re} & -1 \\ 0 & -\frac{2}{Re} \end{pmatrix} \begin{pmatrix} v \\ \eta \end{pmatrix}, \quad (2.11)$$

where Re refers to the Reynolds number. The toy model has negative eigenvalues, $(\lambda_1, \lambda_2) = (-1/Re, -2/Re)$, and unit eigenvectors $\mathbf{x}_1 = (1, 0)$, $\mathbf{x}_2 = \frac{1}{\sqrt{Re^2+1}}(Re, 1)$. Judging from the negative eigenvalues, we conclude that $\mathbf{q}(t)$ will decay exponentially. However, as $Re \rightarrow \infty$, they become increasingly non-orthogonal approaching each other such that the angle between \mathbf{x}_1 and \mathbf{x}_2 tends towards 0. At $Re = 15$, the eigenvector pairs, \mathbf{x}_1 and \mathbf{x}_2 , are highly non-orthogonal, becoming almost linearly dependent shown in figure 2.4(a). For a randomly selected initial condition with an energy-norm of $\|\mathbf{q}_0\|_2 = 15$, where $\|\cdot\|_2$ refers to the L2-norm, the trajectory in green decays exponentially for $t \in [0, 100]$ in figure 2.4(b). In contrast, for a specifically chosen initial condition shown as the blue trajectory, $\|\mathbf{q}\|_2$ is amplified nearly four times before decaying exponentially. The toy model demonstrates the significance of transient growth for a specifically chosen initial condition.

The goal of non-modal stability analysis is to search over all initial conditions, $\tilde{\mathbf{q}}_0$, leading to the maximum amplification factor at time t , resulting in an optimisation problem,

$$G(t) = \max_{\tilde{\mathbf{q}}_0 \neq 0} \frac{\langle \tilde{\mathbf{q}}(t), \tilde{\mathbf{q}}(t) \rangle}{\langle \tilde{\mathbf{q}}_0, \tilde{\mathbf{q}}_0 \rangle}, \quad \text{s.t. } \langle \tilde{\mathbf{q}}_0, \tilde{\mathbf{q}}_0 \rangle = 1, \quad (2.12)$$

where, $\langle \cdot, \cdot \rangle$ refers to the inner-product defined as,

$$\langle \mathbf{x}, \mathbf{y} \rangle = \int_{\Omega} \mathbf{x}^H \mathbf{y} \, d\Omega, \quad (2.13)$$

and \mathbf{x}^H refers to the complex conjugate transpose of \mathbf{x} . By considering the linearised operator of (2.7), we can define a linear time invariant operator given as,

$$\tilde{\mathbf{q}}(t) = \mathcal{A}(t)\tilde{\mathbf{q}}_0, \quad (2.14)$$

which takes the solution from initial conditions, $\tilde{\mathbf{q}}_0$, to $\tilde{\mathbf{q}}(t)$ at time t . Substituting the expression above into equation (2.12),

$$G(t) = \max_{\tilde{\mathbf{q}}_0 \neq 0} \frac{\langle \mathcal{A}(t)\tilde{\mathbf{q}}_0, \mathcal{A}(t)\tilde{\mathbf{q}}_0 \rangle}{\langle \tilde{\mathbf{q}}_0, \tilde{\mathbf{q}}_0 \rangle} = \langle \tilde{\mathbf{q}}_0, \mathcal{A}^\dagger(t)\mathcal{A}(t)\tilde{\mathbf{q}}_0 \rangle = \lambda_{max}(\mathcal{A}^\dagger \mathcal{A}) \quad (2.15)$$

where $\mathcal{A}^\dagger(t)$ refers to the adjoint of $\mathcal{A}(t)$. The maximum amplification factor $\max G(t)$ is the largest eigenvalue, λ_{max} , of $\mathcal{A}^\dagger \mathcal{A}$, and the eigenvalue problem is given as,

$$\mathcal{A}^\dagger(t)\mathcal{A}(t)\tilde{\mathbf{q}}_0 = \lambda \tilde{\mathbf{q}}_0, \quad (2.16)$$

where $\tilde{\mathbf{q}}_0$ refers to the eigenvector denoting the optimal initial condition. For a detailed derivation of the optimal initial conditions or forcing, the reader is referred to [Butler and Farrell, 1992, Schmid, 2007]. An alternative method of computing transient growth is computing the pseudospectral of linear operators discussed in [Trefethen, 1997], outside the scope of this thesis.

Both two-dimensional, $\beta = 0$, and three-dimensional, $\beta \neq 0$, non-modal stability analysis have been studied.

In the two-dimensional form, the optimal initial conditions are in the form of near wall vortices tilted upstream, transiently energised referred to as the Orr-mechanism [Orr, 1907, Farrell, 1988, Reddy

et al., 1993]. In the three-dimension form, streamwise vortices, acting as optimal initial conditions lead to the optimal response in the form of streamwise streaks [Reddy and Henningson, 1993]. Contrary to linear stability analysis which confers two-dimensional perturbations as linearly unstable, the key result in this analysis is that three-dimensional initial conditions, $\alpha = 0$, confer the optimal initial conditions leading to large transient growth at subcritical Reynolds numbers. Figure.. shows this.

The width of the streaks happen to be robustly occur around 100 wall units, the characteristics spacing identified in many experiments [Kline, Panton, Bandybopobi]

The optimal initial conditions involve streamwise vortices which amplify streaks, related to the lift-up effect [Ellingsen and Palm, 1975, Brandt, 2014]. These modal and nonmodal mechanisms above highlight developments based on linear methods.

2.2.2 Nonlinear dynamical systems

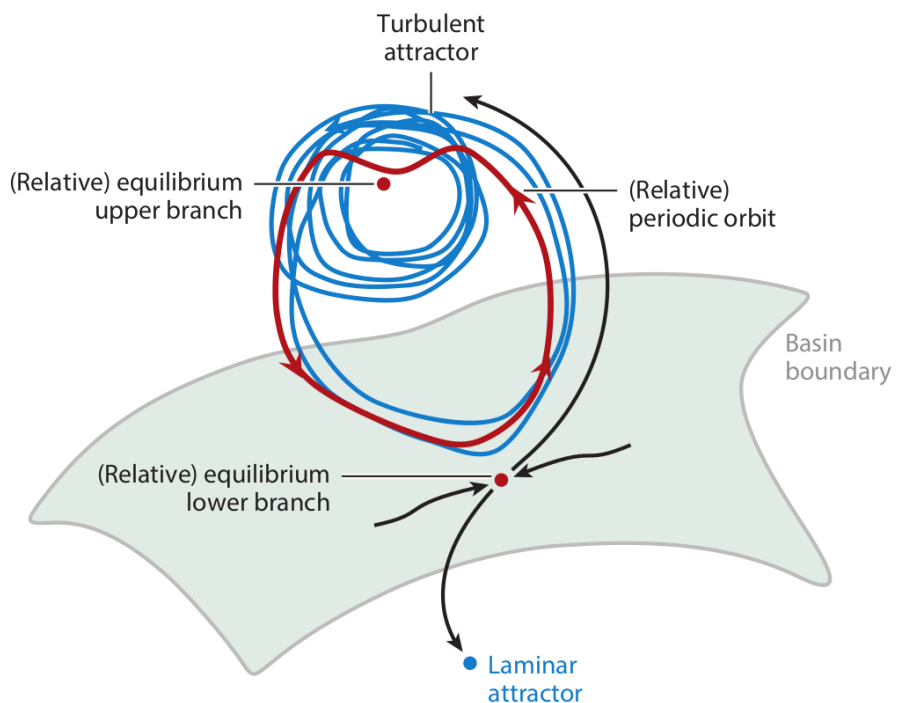


Figure 2.5: The state space organising of the upper and lower branch. Turbulence is interpreted as solution trajectories wander around the upper branch, orbiting around a network unstable invariant states. The lower branch acts as a boundary between the turbulent attractor and laminar attractor, an attractor on the edge referred to as the edge state. Taken from [Graham and Floryan, 2021].

It is well established that coherent motions defined by flow patterns that persist in space and time play an important role in the transport of momentum and heat. In parallel shear flows, these coherent structures typically appear as near-walls streaks and quasi-streamwise rollers. A persistent, quasi-periodic cycle between the regeneration of streaks and rolls, referred to as the *self-sustaining process*, appears to be a fundamental mechanism in sustaining wall-bounded turbulence *self-sustaining process* [Hamilton et al., 1995]. This mechanism is described by the generation of streaks due to quasi-streamwise rollers by redistributing the mean. These streaks become linearly unstable and breakdown, and through a nonlinear process regenerates the quasi-streamwise rollers, closing the cycle.

In the previous section, we have examined the transition process based linear mechanisms. While

such mechanisms are important, the transition to turbulence is ultimately governed fully nonlinear nature of the Navier-Stokes equations. As a result, an increasing attention has been directed towards the description of turbulence as a nonlinear dynamical systems. In this view, turbulence is interpreted as a solution trajectory evolving through a phase space composed of a network such non-trivial nonlinear solutions, commonly referred to as exact coherent states (ECS) or invariant solutions [Graham and Floryan, 2021]. These invariant solutions commonly take the form of as equilibria, travelling waves, periodic and relative periodic orbits.

In the context of parallel shear flows, Nagata was the first to discover a pair of unstable equilibrium solutions in plane Couette flow by smoothly following (homotopy) from a Taylor-Couette configuration [Nagata, 1990]. This pair consist of an unstable upper branch and lower branch emerging as a saddle-node bifurcation near $Re \approx 500$, and is disconnected from the stable laminar solution. The lower branch refers to its proximity towards the stable laminar state in phase space. A travelling-wave solution in plane Couette flow also later found by the same author [Nagata, 1997]. A family of equilibrium and travelling waves solutions was found for plane Couette and plane Poiseuille flows under various boundary conditions (i.e. stress-free, slip and no-slip) where identified by [Waleffe, 2001, 2003].

While these unstable solutions demonstrate good agreements with results from DNS such as the spanwise length scales, and mean and fluctuations, they do not capture the dynamical processes. Periodic orbits defined by time-dependent solutions that have been identified in plane Couette flow [Kawahara and Kida, 2001], describing a single regeneration cycle similar to the self-sustaining process. The chaotic trajectories of turbulence have been found to be embedded within invariant solutions and their connections between them known as heteroclinic orbits, offering a robust view of the building-blocks of of turbulence [Gibson et al., 2008, 2009, Viswanath, 2007, Halcrow et al., 2009, Graham and Floryan, 2021]

In the context of this transitional flows, the lower branch solution can be though of separating the turbulent attractor from the laminar state. Its an attractor that resides on the edge of turbulence, defined as an edge state. The graphical representation of this edge is shown in figure 2.5.

2.2.3 Spatiotemporal transitional flows

This section describes the inherent spatiotemporal intermittent description of turbulence in transitional wall-bounded shear flows commonly reported in large extended domains where the span is about fifty times the half-height of a plane Poiseuille channel, $L/h \gtrsim 50$. In this regime, turbulence is characterised by the coexistence of turbulent and laminar structures. Examples of such are found in canonical shear flow systems such as plane Couette flows [Prigent et al., 2003, Barkley and Tuckerman, 2005, 2007, Tuckerman and Barkley, 2011, Duguet et al., 2010, Reetz et al., 2019], Taylor-Couette flows [Prigent and Dauchot, 2002, Prigent et al., 2003], pipe flows [Avila et al., 2010, 2011, Song et al., 2017, Avila et al., 2023] and plane Poiseuille flows [Tsukahara et al., 2014a,c, Tuckerman et al., 2014, Tsukahara et al., 2014b, Gomé et al., 2020, Paranjape, 2019, Paranjape et al., 2020, 2023].

We will focus on the plane Poiseuille flow configuration, where the spatiotemporal intermittent patterns are referred to as oblique turbulent-laminar bands illustrated in figure 2.6 at $Re = 1400$ for $L/h = 16\pi$. The the bright and dark regions highlights coexisting spatially localised turbulent and laminar regions. These turbulent-laminar bands occur over a range of Reynolds numbers, and its precise range is likely dependent on the domain's aspect ratio [Tsukahara et al., 2014b, Tuckerman et al., 2014, Paranjape et al., 2023]. Near the upper Re threshold of this regime, the domain is

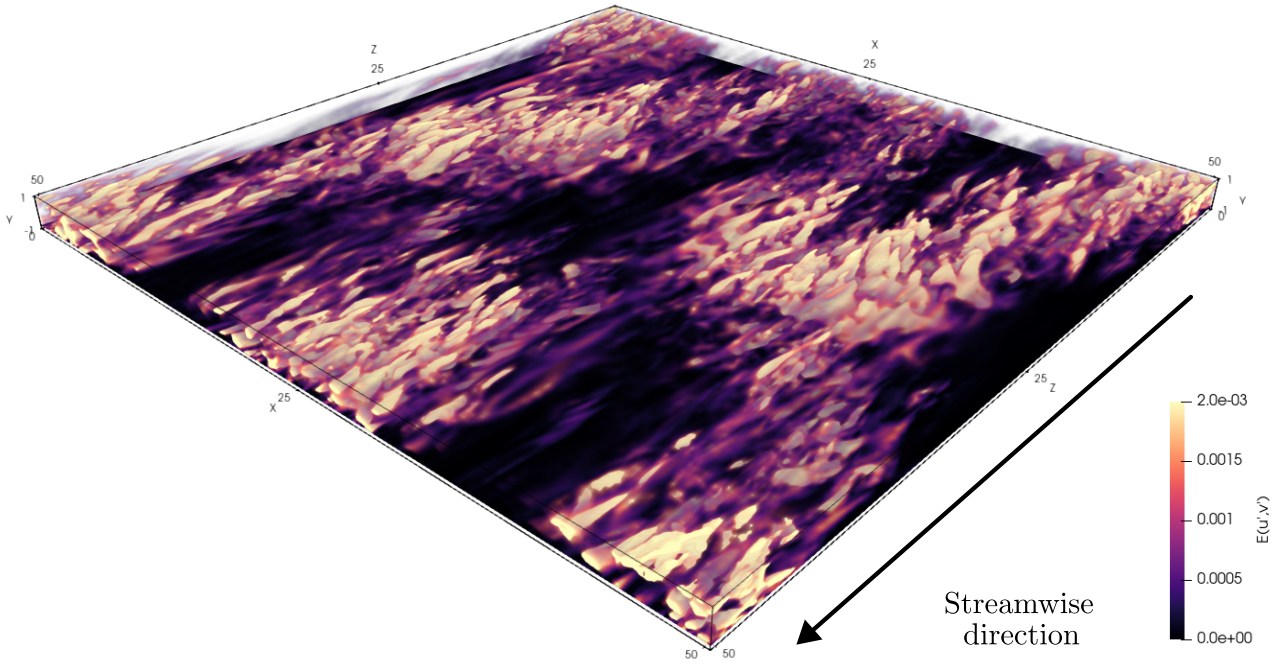


Figure 2.6: A snapshot of turbulent-laminar bands at $Re = 1400$ in a large domain $L/d = 8\pi$, depicting its spatiotemporal intermittent nature. Isovolumetric renderings are based on the spanwise, u' , and wall-normal, v' , perturbation kinetic energy, $E(u', v') = 1/2(u'^2 + v'^2)$, where the perturbation velocities are defined about the laminar state $\mathbf{u}'(\mathbf{x}, t) = \mathbf{u}(\mathbf{x}, t) - U_{lam}(y)$.

fully engulfed by developed turbulent regions, referred to uniform, featureless turbulence appearing at $Re = 1800$ in figure 2.6(a). As Re decreases towards $Re = 1050$, turbulent-laminar bands persist in figures 2.7(b-f). In this region, turbulent-laminar bands angles have been observed to be inclined between $20^\circ \sim 30^\circ$, with streamwise wavelengths of $\sim 60h$, and spanwise wavelengths of $\sim 20h - 30h$ [Tsukahara et al., 2014b]. To study the preference of angles, zzz performed linear stability analysis of bands and showed that preferred angle at .. degrees. Below certain Re threshold, the spatially turbulent regions spontaneously decay where the flow relaminarises asymptotically [Tuckerman et al., 2014]. This decay is shown in $Re = 1000$ near $t = 1600$ in figure 2.7(g).

Inspired from previous studies of turbulent-laminar bands in plane Couette flows [Barkley and Tuckerman, 2005, Reetz et al., 2019], narrow domains, tilted orthogonally to the band angles were considered to investigate their dynamics [Tuckerman et al., 2014, Paranjape et al., 2020, 2023]. In narrow-tilted domains inclined at 24° , the turbulent-bands convect at about $\sim 1\%$ of the bulk velocity, propagating either upstream or downstream, above or below a critical $Re \sim 1000$, independent of domain sizes for $L_z \geq 100h$ [Tuckerman et al., 2014, Gomé et al., 2020]. The characteristic spanwise wavelengths of turbulent-laminar bands are dependent on Re , appearing at $\lambda_z \sim 20h$ for $Re \geq 1400$ and $\lambda_z \sim 40h$ for $Re \leq 1100$. Indeed, between $1300 < Re < 1400$ the bands appear to alternate between two different band-widths [Tuckerman et al., 2014], merging and splitting continuously. This points towards a band splitting event in between $Re = 1100$ and $Re = 1400$, reminiscent of a puff

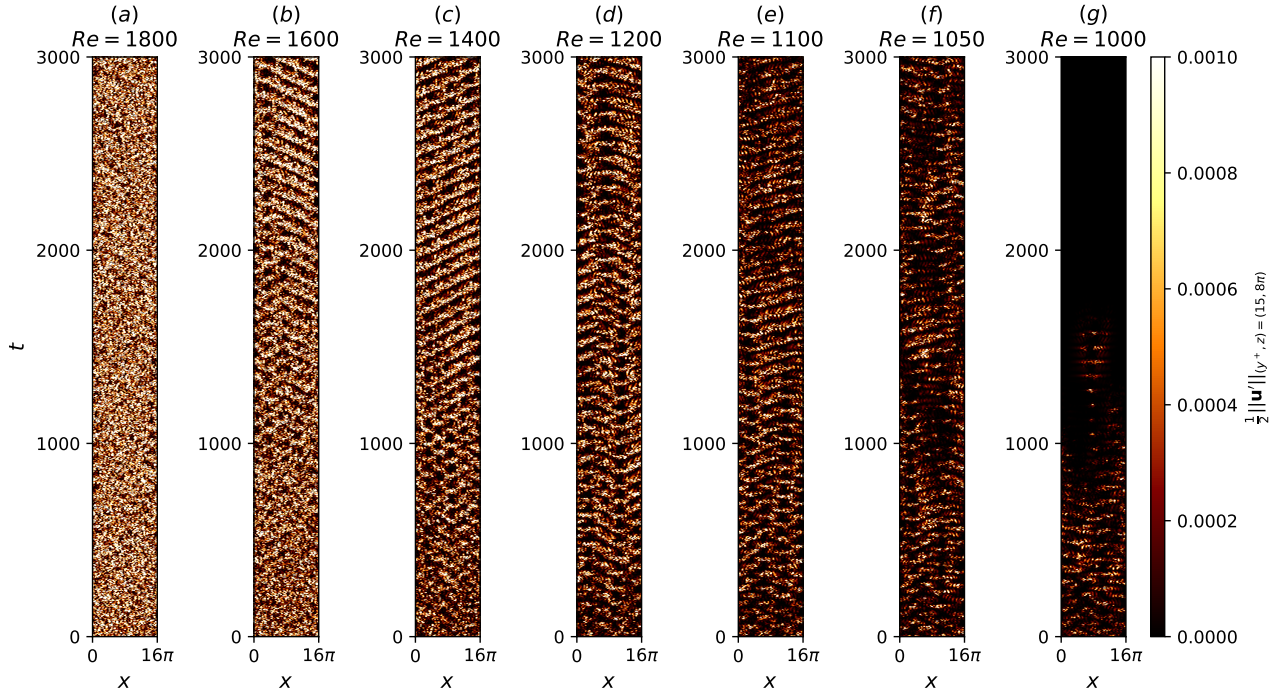


Figure 2.7: Turbulent-laminar bands for $t \in [0, 3000]$ in large domains $(L_x, L_z) = (16\pi, 16\pi)$ at (a) $Re = 1800$, (b) $Re = 1600$, (c) $Re = 1400$, (d) $Re = 1200$, (e) $Re = 1100$, (f) $Re = 1050$, (g) $Re = 1000$.

splitting in pipe flows [Avila et al., 2011].

On the other hand, turbulent bands appear to decay at $Re = 830$ [Gomé et al., 2020], and at $re = 1100$ but surviving for $re = 1000$ [Tuckerman et al., 2014], suggesting that turbulent bands decay spontaneously. [Gomé et al., 2020] computed the probabilities distributions of turbulent band decay, $P(\Delta t^d)$, where Δt^d refers to the time it takes for decay. One of the key insight is that the probability distributions of turbulent band decay mimicks a memoryless Poisson distribution,

$$P(\Delta t^d) = \exp(-\Delta t^d/\tau^d(Re)), \quad (2.17)$$

where $\tau^d(Re)$ refers to the mean lifetime for decay as a function of Re . Similarly, the probability distribution for band splitting also follows a Poisson distribution, $P(\Delta t^s) = \exp(-\Delta t^s/\tau^s(Re))$, where $\tau^s(Re)$ refers to the mean lifetime of a splitting event dependent on Re . The mean survival lifetime of a band decaying, τ^d , and splitting, τ^s , depends superexponentially on Re , i.e. $\tau^{d,s} = \exp(\exp(Re))$. This superexponential dependence is presented in figure 2.8, with a crossover point at $Re_{cross} \approx 965$. This crossover point refers to equal mean survival lifetime of a band suggesting a critical Re for the onset of turbulent bands. While there has been substantial progress made towards understanding the behaviour of periodic turbulent-laminar bands in narrow-tilted domains, recent studies of isolated turbulent bands (ITBs) indicate different behaviour. Notably, ITBs persist at $Re \approx 700$ for $t = 10000$ (far beyond figure 2.8, characterised by streak generating head, and a diffusive upstream tail. [Xiong et al., 2015, Tao et al., 2018, Shimizu and Manneville, 2019, Xiao and Song, 2020]).

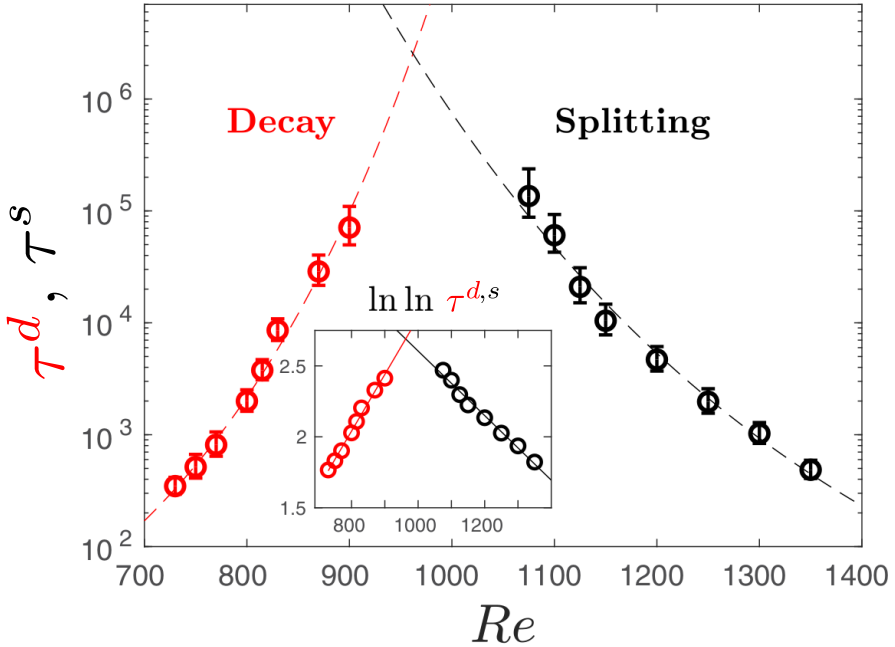


Figure 2.8: The mean decay times (red), τ^d , and mean splitting times (black), τ^s , as a function of Reynolds number, leading to a crossover point at $Re \approx 965$, adapted from [Gomé et al., 2020].

2.3 Rayleigh-Bénard convection (RBC)

Rayleigh-Bénard convection serves as one of the paradigmatic fluid configuration for studying the dynamics of natural convection. The two basic physical mechanisms that underpins RBC is the competition between buoyancy due to heating, and resistance due to viscous forces. As the bottom plate is heated, the bottom layer fluid becomes more buoyant and tends to rise, while the colder top fluid layer is becomes relatively less buoyant and tends to sink, leading to an overturning of layers. Viscous forces between adjacent fluid parcels act to resist the motion. As buoyancy overcomes these viscous forces, the fluid layers overturn, resulting in the initiation of convection. One of the earliest experimental work is performed by Henri Bénard [Bénard, 1901], who observed the onset of hexagonal convection cells above a certain threshold of ΔT . To quantify the ratio between buoyancy and viscous forces, Lord Rayleigh [Rayleigh, 1916] introduced the Rayleigh number, Ra , and predicted the onset of convection at a critical Rayleigh number of $Ra_c = \frac{27}{4}\pi^4 = 657.5$, with a critical wavenumber of $q_c = \frac{\pi}{\sqrt{2}d}$. His work formed the earliest record of linear stability analysis of convection.

The pioneering work from Rayleigh, and Bénard's experiment formed the early foundations of buoyancy-driven convection, now known as Rayleigh-Bénard convection. However, it is worth highlighting the key differences between Bénard's experiment and Rayleigh's analysis. In Bénard's experiments, he considered a thin layer of fluid heated which is freely exposed to ambient air, leading to the formation of hexagonal convection patterns. Unbeknownst to him at that time was that surface tension (Maragoni) effects are important in thin layers of fluid. As fluids in thin layers are being heated, surface tension decreases, generated a tangential forces towards regions of higher surface tension at the surface, where cold fluid resides, amplifying convection, now known as Bénard-Maragoni convection [Manneville, 2006]. In Bénard's case, the effect of surface tension becomes important as the layer of fluid becomes thinner, forming hexagonal cells instead of concentric rolls in thicker layers shown by Hoard et al. [1970].

In the absence of surface tension effects, the critical Rayleigh number, Ra_c depends on the bound-

ary condition, commonly analysed using stress-free or rigid-rigid (no-slip) boundary conditions. In Rayleigh's work, he considered a stress-free condition at the wall, $\partial u / \partial n = 0$, where analytical solutions are admittable. The critical Rayleigh number for the rigid-rigid (no-slip) case is at $Ra_c = 1707.8$ and $q_c = 3.12/d$ (or $\lambda_c \approx 2d$), computed later by Pellew and Southwell [1940], and is independent of Pr [Bodenschatz et al., 2000]. Notably, the size of a single convection roll in the rigid-rigid case, $l_{roll} = 1/2\lambda_c \approx d$, suggesting that the distance separating the two plates dictates the length scale of the convection roll. In this work, I will investigate RBC with no-slip velocity boundary conditions, herein referred to RBC for the rest of the thesis.

Slightly above the onset of convection, described using the reduced Rayleigh number $\varepsilon = (\frac{Ra}{Ra_c} - 1)$, a set of stable convection rolls near q_c are found to exist (CITATIONS?). The theoretical foundations of performing stability analysis using expansion in powers of amplitude (*weakly nonlinear analysis*) was considered by Eckhaus [1965], in which he applied it to the problem of parallel shear flows. The important contribution was that slightly above the onset, stable stationary rolls are found within the range of $Ra > Ra_c + 3\eta(\alpha - \alpha_c)^2$, where $\eta = \frac{1}{2} \frac{\partial Ra}{\partial \alpha}|_{Ra_c}$. Busse and Whitehead [1971] then extended the same technique to Rayleigh-Bénard convection, in which η was found to depend on Pr . Whilst this technique is useful in detailing the stability regions of stationary rolls, it appears to be limited as it contradict some experiments in which time-dependent oscillatory rolls were discovered [Rossby, 1969, Willis and Deardorff, 1970], which has been found to be a secondary instability of stationary convection rolls with complex eigenvalues. As noted by Busse [1972], the applicability of weakly nonlinear analysis is limited to small ε . This limitation is addressed by using directly computing the linear stability of saturated convection rolls computed based on a Galerkin truncation and a root-finding algorithm. The results from linear stability analysis led to the well known Busse balloon which described the stability boundary of the convection rolls in the two dimensional space of $\varepsilon - q$, known as the Busse balloon [Busse, 1978] (figure 2.9).

While the Busse balloon describes the stability boundaries of ISRs over a range of wavenumbers, predicting the wavenumber of an ISR state remains an central challenge [Bodenschatz et al., 2000]. Indeed, experimental investigations of RBC in moderate domain sizes ($\Gamma \geq 7$, where Γ refers to the domain's aspect ratio) in rectangular (straight rolls) and cylindrical (concentric rolls) domains showed that the wavenumbers are confined within the Busse balloon. As ε was continuously modified, the ISRs with wavenumbers that are now outside of the Busse balloon, rolls dislocations and defects spontaneously nucleate, either increasing or decreasing the roll wavenumber, adhering to the the stability boundaries of the Busse balloon. The hysteretic nature of the system implies that the roll wavenumber of the ISRs strongly depends on the system's history [Bodenschatz et al., 2000].

To complicate the subject further, ISRs appear to be an exception rather than the rule [Croquette, 1989b] as multiple 'non-ISR' states, in the form os squares, travelling/stationary targets, giant rotating spirals and oscillatory convection patterns have been found over the years [Croquette, 1989a,b, Plapp et al., 1998, Hof et al., 1999, Rüdiger and Feudel, 2000, Borońska and Tuckerman, 2010a,b]. For example, investigations of cylindrical RBC in small aspect-ratio revealed eight stationary statesand two oscillatory states. These findings were later supported by numerical experiments and bifurcation analyses.

1. Saturated States
2. Busse balloon for $Pr = 1$
3. Skew-varicose, Eckhaus, Cross-roll instabilities

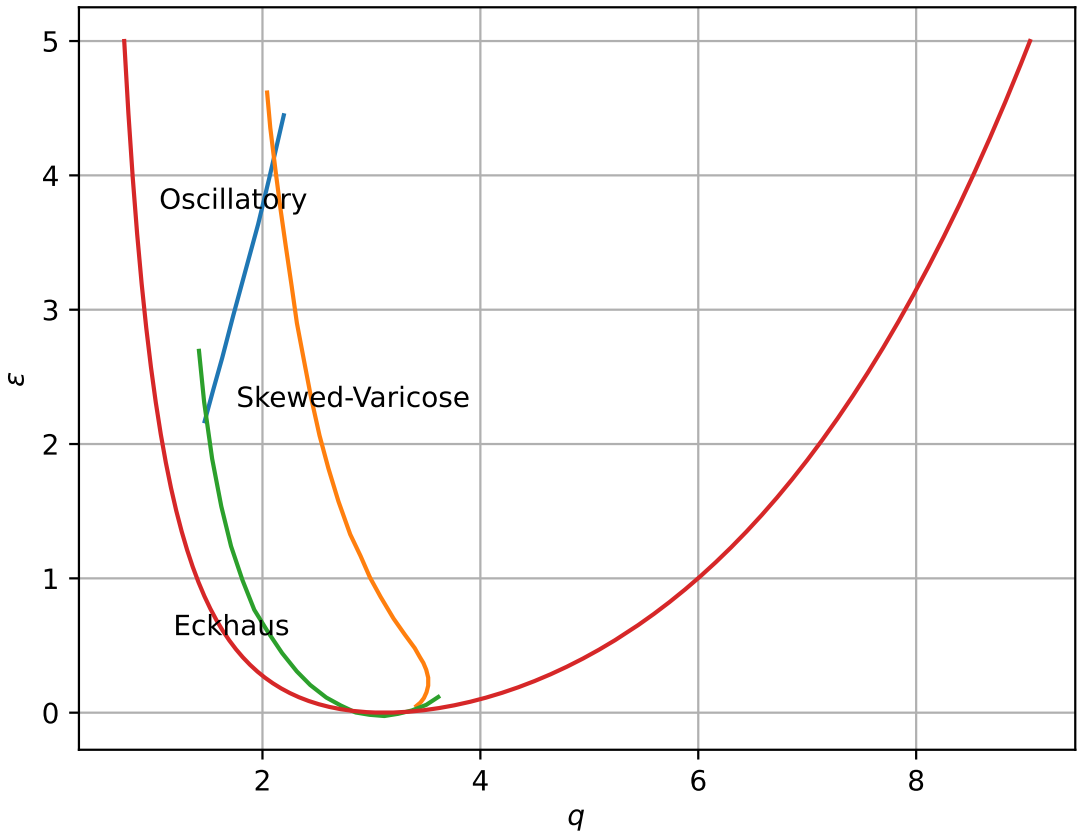


Figure 2.9: The Busse balloon describes the stability boundaries of ISRs in a $\varepsilon - q$ space. For larger wavenumbers, the instability mechanism is described by the skewed-varicose (SV) instability. For smaller wavenumbers, the instability mechanism is described by the Eckhaus instability. For large ε , the instability is described by the onset of oscillatory instability. Busse balloon digitised from [Plapp, 1997] for $Pr \approx 1$

4. Low Pr and high Pr .
5. What happens above the Busse balloon?
 1. Statisitical description of spatial-temporal chaos (i.e correlation length, time etc..)
 2. Challenge with quantifying the onset

2.4 Rayleigh-Bénard Poiseuille (RBP) flows

Gage and Reid [1968] first investigated the primary instabilities of RBP flows, which can be determined by Re , Ra , Pr , and the planar x - z perturbations wavenumbers α, β respectively. For a given Ra and Pr , the neutral stability curves are limited by the development of Tollmien-Schlichting waves for $Re \geq Re_{TS} = 5772.22$ [Orszag, 1971], and convection rolls within $0 \leq Re < Re_{TS}$. Convection rolls can be categorised based on their orientation to the mean flow, namely, longitudinal ($\alpha = 0, \beta \neq 0$), transverse ($\alpha \neq 0, \beta = 0$) and oblique rolls ($\alpha \neq 0, \beta \neq 0$). The linearised system governing the onset of longitudinal rolls is analogous to the linearised RBC system, with a critical Rayleigh number, $Ra_{\parallel} = Ra_{RB} = 1708.8$ and critical wavenumber, $\alpha_{\parallel} = \alpha_{RB} = 3.13$ [Pellew and Southwell, 1940, Kelly, 1994], independent of Re and Pr . The critical Rayleigh number for oblique and transverse rolls matches that of RBC at $Re = 0$ due to horizontal isotropy, but increases as Re increases, depending on Pr , i.e., $Ra_{\perp} = f(Re, Pr)$ [Gage and Reid, 1968, Müller et al., 1992, Nicolas et al., 1997]. When spatially developing instabilities are considered, longitudinal rolls are always convectively unstable, and transverse rolls can become absolutely unstable [Müller et al., 1989, 1992, Carrière and Monkewitz, 1999]. Nonmodal stability analyses of subcritical RBP indicate that the optimal transient growth G_{max} increases gradually with Ra . The wavenumber of the optimal initial conditions, β_{max} , resembles that observed in shear flows [Reddy and Henningson, 1993], and gradually approaches the critical wavenumber of convection rolls, α_{\parallel} , as Ra increases [John Soundar Jerome et al., 2012]. For $Re > 0$, the longitudinal rolls appear as the dominant primary instability [Gage and Reid, 1968]. Secondary stability analyses of longitudinal rolls reveal a wavy instability near $Re \sim 100$ [Clever and Busse, 1991], leading to wavy longitudinal rolls, which are convectively unstable [Pabiou et al., 2005, Nicolas et al., 2010]. The influence of finite lateral extensions in RBP flows on the stability of longitudinal and transverse rolls [Kato and Fujimura, 2000, Nicolas et al., 2000], as well as wavy rolls [Xin et al., 2006, Nicolas et al., 2010], has been reported. In finite streamwise extensions of RBP flows, the onset of convection rolls and the heat flux variations due to entrance effects have been investigated [Mahaney et al., 1988, Lee and Hwang, 1991, Nonino and Giudice, 1991]. More recently, shear-driven turbulence can enhance heat fluxes in turbulent RBP flows [Scagliarini et al., 2014, 2015, Pirozzoli et al., 2017]. RBP flows with sinusoidal heating and wavy walls have also been studied [Hossain et al., 2021]. For an in-depth discussion of RBP flows, see the reviews by Kelly [1994] and Nicolas [2002].

2.4.1 Thesis Outline

In this thesis, I am particularly focused on the transition behaviour of fluid flow driven by shear and buoyancy, addressing questions related to the onset of instabilities due to shear and buoyancy, and the (possible) competitive between shear and buoyancy driven instabilities. I would like to preface that while this thesis is dealing with onset of instabilities, it does not clearly indicate that the onset of such instabilities necessarily lead to turbulence, hence, for terminology sake, we shall be looking into

transitional regimes where the fluid neither laminar nor turbulent. The main motivations are two-folds, both from an academic and applied point-of-view. Within academia, the onset and transition to turbulence in Rayleigh-Bénard Poiseuille flows remains poorly understand. Whilst there had been significant progress in our understand of transition to turbulence in independent setups, Rayleigh-Bénard convection and plane Poiseuille flows, their combined effects are not known. The thesis is structured into the follow, Chapter 1 is the introduction with literature review, chapter 2 methodology assosicated with the spectral/*hp*-element method, chapter 3 with results related to the the Rayleigh and Reynolds number sweep, chapter 4 with a specific focus on the bistability between spiral defect chaos and ideal straight rolls and finally chapter 5 with concluding remarks.

1. Academic motivation - flow structures, statistics, transition.
2. Application motivation - shear, heat transfer. Chip cooling, thin-film fabrication and atmospheric boundary layer.

We seek to investigate the influence of unstable stratification quantified by Rayleigh number Ra , on the behaviour tuburlent-laminar bands. The onset of convection occurs at a critical Rayleigh number of $Ra_c > 1708$, in the form of a pair of convection rolls. When aligned in the streamwise direction, the convection rolls are seemingly analogous to a pair of counter-rotating vortices, an optimal initial condition for transient growth. Our investigation naturally answers a few questions related to turbulent-laminar bands. For example, does the onset of turbulent-laminar bands, Re_{cr} decrease with increasing Ra ? Do Ra -effects influence the structure of turbulent-laminar bands i.e band angle/width?

The answers to our research will have important implications Rayleigh-Bénard Poiseuille flows, ubiquitous in atmospheric, geophysical and engineering flows.

Bibliography

Clouds streets and comma clouds near svalbard. <https://earthobservatory.nasa.gov/images/87749/clouds-streets-and-comma-clouds-near-svalbard>.

Kerstin Avila, David Moxey, Alberto De Lozar, Marc Avila, Dwight Barkley, and Björn Hof. The Onset of Turbulence in Pipe Flow. *Science*, 333(6039):192–196, July 2011. ISSN 0036-8075, 1095-9203. doi: 10.1126/science.1203223. URL <https://www.science.org/doi/10.1126/science.1203223>.

Marc Avila, Ashley P. Willis, and Björn Hof. On the transient nature of localized pipe flow turbulence. *Journal of Fluid Mechanics*, 646:127–136, March 2010. ISSN 0022-1120, 1469-7645. doi: 10.1017/S0022112009993296. URL https://www.cambridge.org/core/product/identifier/S0022112009993296/type/journal_article.

Marc Avila, Dwight Barkley, and Björn Hof. Transition to Turbulence in Pipe Flow. *Annual Review of Fluid Mechanics*, 55(1):575–602, January 2023. ISSN 0066-4189, 1545-4479. doi: 10.1146/annurev-fluid-120720-025957. URL <https://www.annualreviews.org/doi/10.1146/annurev-fluid-120720-025957>.

Dwight Barkley and Laurette S. Tuckerman. Computational Study of Turbulent Laminar Patterns in Couette Flow. *Physical Review Letters*, 94(1):014502, January 2005. doi: 10.1103/PhysRevLett.94.014502. URL <https://link.aps.org/doi/10.1103/PhysRevLett.94.014502>. Publisher: American Physical Society.

Dwight Barkley and Laurette S Tuckerman. Mean flow of turbulent-laminar patterns in plane Couette flow. *Journal of Fluid Mechanics*, 576:109–137, 2007. ISSN 1469-7645. Publisher: Cambridge University Press.

Eberhard Bodenschatz, Werner Pesch, and Guenter Ahlers. Recent Developments in Rayleigh-Bénard Convection. *Annual Review of Fluid Mechanics*, 32(1):709–778, January 2000. ISSN 0066-4189, 1545-4479. doi: 10.1146/annurev.fluid.32.1.709. URL <https://www.annualreviews.org/doi/10.1146/annurev.fluid.32.1.709>.

Katarzyna Borońska and Laurette S. Tuckerman. Extreme multiplicity in cylindrical Rayleigh-Bénard convection. I. Time dependence and oscillations. *Physical Review E*, 81(3):036320, March 2010a. ISSN 1539-3755, 1550-2376. doi: 10.1103/PhysRevE.81.036320. URL <https://link.aps.org/doi/10.1103/PhysRevE.81.036320>.

Katarzyna Borońska and Laurette S. Tuckerman. Extreme multiplicity in cylindrical Rayleigh-Bénard convection. II. Bifurcation diagram and symmetry classification. *Physical Review E*, 81(3):036321, March 2010b. ISSN 1539-3755, 1550-2376. doi: 10.1103/PhysRevE.81.036321. URL <https://link.aps.org/doi/10.1103/PhysRevE.81.036321>.

Luca Brandt. The lift-up effect: The linear mechanism behind transition and turbulence in shear flows. *European Journal of Mechanics - B/Fluids*, 47:80–96, September 2014. ISSN 09977546. doi: 10.1016/j.euromechflu.2014.03.005. URL <https://linkinghub.elsevier.com/retrieve/pii/S0997754614000405>.

F. H. Busse. The oscillatory instability of convection rolls in a low Prandtl number fluid. *Journal of Fluid Mechanics*, 52(1):97–112, March 1972. ISSN 0022-1120, 1469-7645. doi: 10.1017/S0022112072002988. URL https://www.cambridge.org/core/product/identifier/S0022112072002988/type/journal_article.

F H Busse. Non-linear properties of thermal convection. *Reports on Progress in Physics*, 41(12):1929–1967, December 1978. ISSN 0034-4885, 1361-6633. doi: 10.1088/0034-4885/41/12/003. URL <https://iopscience.iop.org/article/10.1088/0034-4885/41/12/003>.

F. H. Busse and J. A. Whitehead. Instabilities of convection rolls in a high Prandtl number fluid. *Journal of Fluid Mechanics*, 47(2):305–320, May 1971. ISSN 0022-1120, 1469-7645. doi: 10.1017/S0022112071001071. URL https://www.cambridge.org/core/product/identifier/S0022112071001071/type/journal_article.

Kathryn M. Butler and Brian F. Farrell. Three-dimensional optimal perturbations in viscous shear flow. *Physics of Fluids A: Fluid Dynamics*, 4(8):1637–1650, August 1992. ISSN 0899-8213. doi: 10.1063/1.858386. URL <https://pubs.aip.org/pof/article/4/8/1637/402702/Three-dimensional-optimal-perturbations-in-viscous>.

Henri Bénard. Les tourbillons cellulaires dans une nappe liquide. - Méthodes optiques d'observation et d'enregistrement. *Journal de Physique Théorique et Appliquée*, 10(1):254–266, 1901. ISSN 0368-3893. doi: 10.1051/jphystab:0190100100025400. URL <http://www.edpsciences.org/10.1051/jphystab:0190100100025400>.

Philippe Carrière and Peter A. Monkewitz. Convective versus absolute instability in mixed Rayleigh–Bénard–Poiseuille convection. *Journal of Fluid Mechanics*, 384:243–262, April 1999. ISSN 0022-1120, 1469-7645. doi: 10.1017/S0022112098004145. URL https://www.cambridge.org/core/product/identifier/S0022112098004145/type/journal_article.

R. M. Clever and F. H. Busse. Instabilities of longitudinal rolls in the presence of Poiseuille flow. *Journal of Fluid Mechanics*, 229(-1):517, August 1991. ISSN 0022-1120, 1469-7645. doi: 10.1017/S0022112091003142. URL http://www.journals.cambridge.org/abstract_S0022112091003142.

Vincent Croquette. Convective pattern dynamics at low Prandtl number: Part I. *Contemporary Physics*, 30(2):113–133, March 1989a. ISSN 0010-7514, 1366-5812. doi: 10.1080/00107518908225511. URL <http://www.tandfonline.com/doi/abs/10.1080/00107518908225511>.

Vincent Croquette. Convective pattern dynamics at low Prandtl number: Part II. *Contemporary Physics*, 30(3):153–171, May 1989b. ISSN 0010-7514, 1366-5812. doi: 10.1080/00107518908222594. URL <http://www.tandfonline.com/doi/abs/10.1080/00107518908222594>.

Y. Duguet, P. Schlatter, and D. S. Henningson. Formation of turbulent patterns near the onset of transition in plane Couette flow. *Journal of Fluid Mechanics*, 650:119–129, May 2010. ISSN 0022-

1120, 1469-7645. doi: 10.1017/S0022112010000297. URL https://www.cambridge.org/core/product/identifier/S0022112010000297/type/journal_article.

Wiktor Eckhaus. *Studies in Non-Linear Stability Theory*, volume 6 of *Springer Tracts in Natural Philosophy*. Springer Berlin Heidelberg, Berlin, Heidelberg, 1965. ISBN 978-3-642-88319-4 978-3-642-88317-0. doi: 10.1007/978-3-642-88317-0. URL <http://link.springer.com/10.1007/978-3-642-88317-0>.

T. Ellingsen and E. Palm. Stability of linear flow. *The Physics of Fluids*, 18(4):487–488, April 1975. ISSN 0031-9171. doi: 10.1063/1.861156. URL <https://pubs.aip.org/pfl/article/18/4/487/459138/Stability-of-linear-flow>.

Greg Evans and Ralph Greif. Unsteady three-dimensional mixed convection in a heated horizontal channel with applications to chemical vapor deposition. *International Journal of Heat and Mass Transfer*, 34(8):2039–2051, August 1991. ISSN 00179310. doi: 10.1016/0017-9310(91)90215-Z. URL <https://linkinghub.elsevier.com/retrieve/pii/001793109190215Z>.

Brian F. Farrell. Optimal excitation of perturbations in viscous shear flow. *The Physics of Fluids*, 31(8):2093–2102, August 1988. ISSN 0031-9171. doi: 10.1063/1.866609. URL <https://pubs.aip.org/pfl/article/31/8/2093/966463/Optimal-excitation-of-perturbations-in-viscous>.

K. S. Gage and W. H. Reid. The stability of thermally stratified plane Poiseuille flow. *Journal of Fluid Mechanics*, 33(1):21–32, July 1968. ISSN 0022-1120, 1469-7645. doi: 10.1017/S0022112068002326. URL https://www.cambridge.org/core/product/identifier/S0022112068002326/type/journal_article.

J. F. Gibson, J. Halcrow, and P. Cvitanović. Visualizing the geometry of state space in plane Couette flow. *Journal of Fluid Mechanics*, 611:107–130, September 2008. ISSN 0022-1120, 1469-7645. doi: 10.1017/S002211200800267X. URL https://www.cambridge.org/core/product/identifier/S002211200800267X/type/journal_article.

J. F. Gibson, J. Halcrow, and P. Cvitanović. Equilibrium and travelling-wave solutions of plane Couette flow. *Journal of Fluid Mechanics*, 638:243–266, November 2009. ISSN 0022-1120, 1469-7645. doi: 10.1017/S0022112009990863. URL https://www.cambridge.org/core/product/identifier/S0022112009990863/type/journal_article.

Sébastien Gomé, Laurette S. Tuckerman, and Dwight Barkley. Statistical transition to turbulence in plane channel flow. *Physical Review Fluids*, 5(8):083905, August 2020. ISSN 2469-990X. doi: 10.1103/PhysRevFluids.5.083905. URL <https://link.aps.org/doi/10.1103/PhysRevFluids.5.083905>.

Michael D. Graham and Daniel Floryan. Exact Coherent States and the Nonlinear Dynamics of Wall-Bounded Turbulent Flows. *Annual Review of Fluid Mechanics*, 53(1):227–253, January 2021. ISSN 0066-4189, 1545-4479. doi: 10.1146/annurev-fluid-051820-020223. URL <https://www.annualreviews.org/doi/10.1146/annurev-fluid-051820-020223>.

J. Halcrow, J. F. Gibson, P. Cvitanović, and D. Viswanath. Heteroclinic connections in plane Couette flow. *Journal of Fluid Mechanics*, 621:365–376, February 2009. ISSN 0022-1120, 1469-7645. doi: 10.1017/S0022112008005065. URL https://www.cambridge.org/core/product/identifier/S0022112008005065/type/journal_article.

James M. Hamilton, John Kim, and Fabian Waleffe. Regeneration mechanisms of near-wall turbulence structures. *Journal of Fluid Mechanics*, 287:317–348, March 1995. ISSN 0022-1120, 1469-7645. doi: 10.1017/S0022112095000978. URL https://www.cambridge.org/core/product/identifier/S0022112095000978/type/journal_article.

C.Q Hoard, C.R Robertson, and A Acrivos. Experiments on the cellular structure in bénard convection. *International Journal of Heat and Mass Transfer*, 13(5):849–856, May 1970. ISSN 00179310. doi: 10.1016/0017-9310(70)90130-4. URL <https://linkinghub.elsevier.com/retrieve/pii/0017931070901304>.

B. Hof, P. G. J. Lucas, and T. Mullin. Flow state multiplicity in convection. *Physics of Fluids*, 11(10):2815–2817, October 1999. ISSN 1070-6631, 1089-7666. doi: 10.1063/1.870178. URL <https://pubs.aip.org/pof/article/11/10/2815/254396/Flow-state-multiplicity-in-convection>.

Mohammad Z. Hossain, Chris D. Cantwell, and Spencer J. Sherwin. A spectral/ hp element method for thermal convection. *International Journal for Numerical Methods in Fluids*, 93(7):2380–2395, July 2021. ISSN 0271-2091, 1097-0363. doi: 10.1002/fld.4978. URL <https://onlinelibrary.wiley.com/doi/10.1002/fld.4978>.

Klavs F. Jensen, Erik O. Einset, and Dimitrios I. Fotiadis. Flow Phenomena in Chemical Vapor Deposition of Thin Films. *Annual Review of Fluid Mechanics*, 23(1):197–232, January 1991. ISSN 0066-4189, 1545-4479. doi: 10.1146/annurev.fl.23.010191.001213. URL <https://www.annualreviews.org/doi/10.1146/annurev.fl.23.010191.001213>.

J. John Soundar Jerome, Jean-Marc Chomaz, and Patrick Huerre. Transient growth in Rayleigh-Bénard-Poiseuille/Couette convection. *Physics of Fluids*, 24(4):044103, April 2012. ISSN 1070-6631, 1089-7666. doi: 10.1063/1.4704642. URL <https://pubs.aip.org/pof/article/24/4/044103/257562/Transient-growth-in-Rayleigh-Benard-Poiseuille>.

Yuki Kato and Kaoru Fujimura. Prediction of pattern selection due to an interaction between longitudinal rolls and transverse modes in a flow through a rectangular channel heated from below. *Physical Review E*, 62(1):601–611, July 2000. ISSN 1063-651X, 1095-3787. doi: 10.1103/PhysRevE.62.601. URL <https://link.aps.org/doi/10.1103/PhysRevE.62.601>.

Genta Kawahara and Shigeo Kida. Periodic motion embedded in plane Couette turbulence: regeneration cycle and burst. *Journal of Fluid Mechanics*, 449:291–300, December 2001. ISSN 0022-1120, 1469-7645. doi: 10.1017/S0022112001006243. URL https://www.cambridge.org/core/product/identifier/S0022112001006243/type/journal_article.

R.E. Kelly. The Onset and Development of Thermal Convection in Fully Developed Shear Flows. In *Advances in Applied Mechanics*, volume 31, pages 35–112. Elsevier, 1994. ISBN 978-0-12-002031-7. doi: 10.1016/S0065-2156(08)70255-2. URL <https://linkinghub.elsevier.com/retrieve/pii/S0065215608702552>.

K.J. Kennedy and A. Zebib. Combined free and forced convection between horizontal parallel planes: some case studies. *International Journal of Heat and Mass Transfer*, 26(3):471–474, March 1983. ISSN 00179310. doi: 10.1016/0017-9310(83)90052-2. URL <https://linkinghub.elsevier.com/retrieve/pii/0017931083900522>.

F.S. Lee and G.J. Hwang. The effect of asymmetric heating on the onset of thermal instability in the thermal entrance region of a parallel plate channel. *International Journal of Heat and Mass Transfer*, 34(9):2207–2218, September 1991. ISSN 00179310. doi: 10.1016/0017-9310(91)90047-I. URL <https://linkinghub.elsevier.com/retrieve/pii/001793109190047I>.

H. V. Mahaney, F. P. Incropera, and S. Ramadhyani. EFFECT OF WALL HEAT FLUX DISTRIBUTION ON LAMINAR MIXED CONVECTION IN THE ENTRANCE REGION OF A HORIZONTAL RECTANGULAR DUCT. *Numerical Heat Transfer*, 13(4):427–450, June 1988. ISSN 0149-5720. doi: 10.1080/10407788808913624. URL <http://www.tandfonline.com/doi/abs/10.1080/10407788808913624>.

Paul Manneville. Rayleigh-Bénard Convection: Thirty Years of Experimental, Theoretical, and Modeling Work. In Gerhard Höhler, Johann H. Kühn, Thomas Müller, Joachim Trümper, Andrei Ruckenstein, Peter Wölfle, Frank Steiner, Innocent Mutabazi, José Eduardo Wesfreid, and Etienne Guyon, editors, *Dynamics of Spatio-Temporal Cellular Structures*, volume 207, pages 41–65. Springer New York, New York, NY, 2006. ISBN 978-0-387-40098-3 978-0-387-25111-0. doi: 10.1007/978-0-387-25111-0_3. URL http://link.springer.com/10.1007/978-0-387-25111-0_3. Series Title: Springer Tracts in Modern Physics.

Á. Meseguer and L.N. Trefethen. Linearized pipe flow to Reynolds number 107. *Journal of Computational Physics*, 186(1):178–197, March 2003. ISSN 00219991. doi: 10.1016/S0021-9991(03)00029-9. URL <https://linkinghub.elsevier.com/retrieve/pii/S0021999103000299>.

H. W Müller, M Lücke, and M Kamps. Convective Patterns in Horizontal Flow. *Europhysics Letters (EPL)*, 10(5):451–456, November 1989. ISSN 0295-5075, 1286-4854. doi: 10.1209/0295-5075/10/5/011. URL <https://iopscience.iop.org/article/10.1209/0295-5075/10/5/011>.

H. W. Müller, M. Lücke, and M. Kamps. Transversal convection patterns in horizontal shear flow. *Physical Review A*, 45(6):3714–3726, March 1992. ISSN 1050-2947, 1094-1622. doi: 10.1103/PhysRevA.45.3714. URL <https://link.aps.org/doi/10.1103/PhysRevA.45.3714>.

M. Nagata. Three-dimensional finite-amplitude solutions in plane Couette flow: bifurcation from infinity. *Journal of Fluid Mechanics*, 217:519–527, August 1990. ISSN 0022-1120, 1469-7645. doi: 10.1017/S0022112090000829. URL https://www.cambridge.org/core/product/identifier/S0022112090000829/type/journal_article.

M. Nagata. Three-dimensional traveling-wave solutions in plane Couette flow. *Physical Review E*, 55(2):2023–2025, February 1997. ISSN 1063-651X, 1095-3787. doi: 10.1103/PhysRevE.55.2023. URL <https://link.aps.org/doi/10.1103/PhysRevE.55.2023>.

X. Nicolas, A. Mojtabi, and J. K. Platten. Two-dimensional numerical analysis of the Poiseuille–Bénard flow in a rectangular channel heated from below. *Physics of Fluids*, 9(2):337–348, February 1997. ISSN 1070-6631, 1089-7666. doi: 10.1063/1.869235. URL <https://pubs.aip.org/pof/article/9/2/337/259822/Two-dimensional-numerical-analysis-of-the>.

X. Nicolas, J.-M. Luijkx, and J.-K. Platten. Linear stability of mixed convection flows in horizontal rectangular channels of finite transversal extension heated from below. *International Journal of Heat and Mass Transfer*, 43(4):589–610, February 2000. ISSN 00179310. doi: 10.1016/S0017-9310(99)00099-X. URL <https://linkinghub.elsevier.com/retrieve/pii/S001793109900099X>.

Xavier Nicolas. Revue bibliographique sur les écoulements de Poiseuille-Rayleigh-Bénard : écoulements de convection mixte en conduites rectangulaires horizontales chauffées par le bas. *International Journal of Thermal Sciences*, 41(10):961–1016, October 2002. ISSN 12900729. doi: 10.1016/S1290-0729(02)01374-1. URL <https://linkinghub.elsevier.com/retrieve/pii/S1290072902013741>.

Xavier Nicolas, Shihe Xin, and Noussaiba Zoueidi. Characterisation of a Wavy Convective Instability in Poiseuille-Rayleigh-Be'nard Flows: Linear Stability Analysis and Non Linear Numerical Simulations Under Random Excitations. In *2010 14th International Heat Transfer Conference, Volume 7*, pages 203–208, Washington, DC, USA, January 2010. ASMEDC. ISBN 978-0-7918-4942-2 978-0-7918-3879-2. doi: 10.1115/IHTC14-22256. URL <https://asmedigitalcollection.asme.org/IHTC/proceedings/IHTC14/49422/203/360332>.

C. Nonino and S. Del Giudice. Laminar mixed convection in the entrance region of horizontal rectangular ducts. *International Journal for Numerical Methods in Fluids*, 13(1):33–48, June 1991. ISSN 0271-2091, 1097-0363. doi: 10.1002/fld.1650130103. URL <https://onlinelibrary.wiley.com/doi/10.1002/fld.1650130103>.

William M'F. Orr. The Stability or Instability of the Steady Motions of a Perfect Liquid and of a Viscous Liquid. Part II: A Viscous Liquid. *Proceedings of the Royal Irish Academy. Section A: Mathematical and Physical Sciences*, 27:69–138, 1907. ISSN 00358975. URL <http://www.jstor.org/stable/20490591>. Publisher: Royal Irish Academy.

Steven A. Orszag. Accurate solution of the Orr-Sommerfeld stability equation. *Journal of Fluid Mechanics*, 50(4):689–703, December 1971. ISSN 0022-1120, 1469-7645. doi: 10.1017/S0022112071002842. URL https://www.cambridge.org/core/product/identifier/S0022112071002842/type/journal_article.

Hervé Pabiou, Sophie Mergui, and Christine Bénard. Wavy secondary instability of longitudinal rolls in RayleighPoiseuille flows. *Journal of Fluid Mechanics*, 542(-1):175, October 2005. ISSN 0022-1120, 1469-7645. doi: 10.1017/S0022112005006154. URL http://www.journals.cambridge.org/abstract_S0022112005006154.

Chaitanya S Paranjape. Onset of turbulence in plane Poiseuille flow. 2019. Publisher: IST Austria Klosterneuburg, Austria.

Chaitanya S. Paranjape, Yohann Duguet, and Björn Hof. Oblique stripe solutions of channel flow. *Journal of Fluid Mechanics*, 897:A7, August 2020. ISSN 0022-1120, 1469-7645. doi: 10.1017/jfm.2020.322. URL https://www.cambridge.org/core/product/identifier/S0022112020003225/type/journal_article.

Chaitanya S. Paranjape, Gökhan Yalnız, Yohann Duguet, Nazmi Burak Budanur, and Björn Hof. Direct Path from Turbulence to Time-Periodic Solutions. *Physical Review Letters*, 131(3):034002, July 2023. ISSN 0031-9007, 1079-7114. doi: 10.1103/PhysRevLett.131.034002. URL <https://link.aps.org/doi/10.1103/PhysRevLett.131.034002>.

Anne Pellew and Richard Vynne Southwell. On maintained convective motion in a fluid heated from below. *Proceedings of the Royal Society of London. Series A. Mathematical and Physical Sciences*,

176(966):312–343, November 1940. ISSN 0080-4630, 2053-9169. doi: 10.1098/rspa.1940.0092. URL <https://royalsocietypublishing.org/doi/10.1098/rspa.1940.0092>.

Sergio Pirozzoli, Matteo Bernardini, Roberto Verzicco, and Paolo Orlandi. Mixed convection in turbulent channels with unstable stratification. *Journal of Fluid Mechanics*, 821:482–516, June 2017. ISSN 0022-1120, 1469-7645. doi: 10.1017/jfm.2017.216. URL https://www.cambridge.org/core/product/identifier/S0022112017002166/type/journal_article.

Brendan B. Plapp, David A. Egolf, Eberhard Bodenschatz, and Werner Pesch. Dynamics and Selection of Giant Spirals in Rayleigh-Bénard Convection. *Physical Review Letters*, 81(24):5334–5337, December 1998. ISSN 0031-9007, 1079-7114. doi: 10.1103/PhysRevLett.81.5334. URL <https://link.aps.org/doi/10.1103/PhysRevLett.81.5334>.

Brendan Bryce Plapp. Spiral pattern formation in Rayleigh-Benard convection. *Ph.D. Thesis*, page 3118, December 1997. URL <https://ui.adsabs.harvard.edu/abs/1997PhDT.....105P>.

A. Prigent and O. Dauchot. "Barber pole turbulence" in large aspect ratio Taylor-Couette flow. *Physical Review Letters*, 89(1):014501, June 2002. ISSN 0031-9007, 1079-7114. doi: 10.1103/PhysRevLett.89.014501. URL <http://arxiv.org/abs/cond-mat/0009241>. arXiv:cond-mat/0009241.

Arnaud Prigent, Guillaume Grégoire, Hugues Chaté, and Olivier Dauchot. Long-wavelength modulation of turbulent shear flows. *Physica D: Nonlinear Phenomena*, 174(1-4):100–113, January 2003. ISSN 01672789. doi: 10.1016/S0167-2789(02)00685-1. URL <https://linkinghub.elsevier.com/retrieve/pii/S0167278902006851>.

Subhashis Ray and J. Srinivasan. Analysis of conjugate laminar mixed convection cooling in a shrouded array of electronic components. *International Journal of Heat and Mass Transfer*, 35(4):815–822, April 1992. ISSN 00179310. doi: 10.1016/0017-9310(92)90249-R. URL <https://linkinghub.elsevier.com/retrieve/pii/001793109290249R>.

Lord Rayleigh. LIX. *On convection currents in a horizontal layer of fluid, when the higher temperature is on the under side. The London, Edinburgh, and Dublin Philosophical Magazine and Journal of Science*, 32(192):529–546, December 1916. ISSN 1941-5982, 1941-5990. doi: 10.1080/14786441608635602. URL <https://www.tandfonline.com/doi/full/10.1080/14786441608635602>.

Satish C. Reddy and Dan S. Henningson. Energy growth in viscous channel flows. *Journal of Fluid Mechanics*, 252:209–238, July 1993. ISSN 0022-1120, 1469-7645. doi: 10.1017/S0022112093003738. URL https://www.cambridge.org/core/product/identifier/S0022112093003738/type/journal_article.

Satish C. Reddy, Peter J. Schmid, and Dan S. Henningson. Pseudospectra of the Orr–Sommerfeld Operator. *SIAM Journal on Applied Mathematics*, 53(1):15–47, February 1993. ISSN 0036-1399, 1095-712X. doi: 10.1137/0153002. URL <http://pubs.siam.org/doi/10.1137/0153002>.

Florian Reetz, Tobias Kreilos, and Tobias M. Schneider. Exact invariant solution reveals the origin of self-organized oblique turbulent-laminar stripes. *Nature Communications*, 10(1):2277, May 2019. ISSN 2041-1723. doi: 10.1038/s41467-019-10208-x. URL <https://doi.org/10.1038/s41467-019-10208-x>.

Osborne Reynolds. XXIX. An experimental investigation of the circumstances which determine whether the motion of water shall be direct or sinuous, and of the law of resistance in parallel channels. *Philosophical Transactions of the Royal Society of London*, 174:935–982, December 1883. ISSN 0261-0523, 2053-9223. doi: 10.1098/rstl.1883.0029. URL <https://royalsocietypublishing.org/doi/10.1098/rstl.1883.0029>.

Osborne Reynolds. IV. On the dynamical theory of incompressible viscous fluids and the determination of the criterion. *Philosophical Transactions of the Royal Society of London. (A.)*, 186:123–164, December 1895. ISSN 0264-3820, 2053-9231. doi: 10.1098/rsta.1895.0004. URL <https://royalsocietypublishing.org/doi/10.1098/rsta.1895.0004>.

H. T. Rossby. A study of Bénard convection with and without rotation. *Journal of Fluid Mechanics*, 36(2):309–335, April 1969. ISSN 0022-1120, 1469-7645. doi: 10.1017/S0022112069001674. URL https://www.cambridge.org/core/product/identifier/S0022112069001674/type/journal_article.

Sten Rüdiger and Fred Feudel. Pattern formation in Rayleigh-Bénard convection in a cylindrical container. *Physical Review E*, 62(4):4927–4931, October 2000. ISSN 1063-651X, 1095-3787. doi: 10.1103/PhysRevE.62.4927. URL <https://link.aps.org/doi/10.1103/PhysRevE.62.4927>.

A. Scagliarini, H. Einarsson, Á. Gylfason, and F. Toschi. Law of the wall in an unstably stratified turbulent channel flow. *Journal of Fluid Mechanics*, 781:R5, October 2015. ISSN 0022-1120, 1469-7645. doi: 10.1017/jfm.2015.498. URL https://www.cambridge.org/core/product/identifier/S002211201500498X/type/journal_article.

Andrea Scagliarini, Armann Gylfason, and Federico Toschi. Heat flux scaling in turbulent Rayleigh-Bénard convection with an imposed longitudinal wind. *Physical Review E*, 89(4):043012, April 2014. ISSN 1539-3755, 1550-2376. doi: 10.1103/PhysRevE.89.043012. URL <http://arxiv.org/abs/1311.4598>. arXiv:1311.4598 [physics].

H. Schlichting. Zur Entstehung der Turbulenz bei der Plattenströmung. *Nachrichten von der Gesellschaft der Wissenschaften zu Göttingen, Mathematisch-Physikalische Klasse*, 1933:181–208, 1933. URL <http://eudml.org/doc/59420>.

Hermann Schlichting and Klaus Gersten. Onset of Turbulence (Stability Theory). In *Boundary-Layer Theory*, pages 415–496. Springer Berlin Heidelberg, Berlin, Heidelberg, 2017. ISBN 978-3-662-52917-1 978-3-662-52919-5. doi: 10.1007/978-3-662-52919-5_15. URL http://link.springer.com/10.1007/978-3-662-52919-5_15.

Peter J. Schmid. Nonmodal Stability Theory. *Annual Review of Fluid Mechanics*, 39(1):129–162, January 2007. ISSN 0066-4189, 1545-4479. doi: 10.1146/annurev.fluid.38.050304.092139. URL <https://www.annualreviews.org/doi/10.1146/annurev.fluid.38.050304.092139>.

Peter J. Schmid and Dan S. Henningson. *Stability and Transition in Shear Flows*, volume 142 of *Applied Mathematical Sciences*. Springer New York, New York, NY, 2001. ISBN 978-1-4612-6564-1 978-1-4613-0185-1. doi: 10.1007/978-1-4613-0185-1. URL <http://link.springer.com/10.1007/978-1-4613-0185-1>.

Masaki Shimizu and Paul Manneville. Bifurcations to turbulence in transitional channel flow. *Physical Review Fluids*, 4(11):113903, November 2019. doi: 10.1103/PhysRevFluids.4.113903. URL <https://link.aps.org/doi/10.1103/PhysRevFluids.4.113903>. Publisher: American Physical Society.

Arnold Sommerfeld. *Ein Beitrag zur hydrodynamischen Erklärung der turbulenten Flüssigkeitsbewegungen*. 1909.

Baofang Song, Dwight Barkley, Björn Hof, and Marc Avila. Speed and structure of turbulent fronts in pipe flow. *Journal of Fluid Mechanics*, 813:1045–1059, February 2017. ISSN 0022-1120, 1469-7645. doi: 10.1017/jfm.2017.14. URL https://www.cambridge.org/core/product/identifier/S0022112017000143/type/journal_article.

Herbert Brian Squire. On the stability for three-dimensional disturbances of viscous fluid flow between parallel walls. *Proceedings of the Royal Society of London. Series A, Containing Papers of a Mathematical and Physical Character*, 142(847):621–628, November 1933. ISSN 0950-1207, 2053-9150. doi: 10.1098/rspa.1933.0193. URL <https://royalsocietypublishing.org/doi/10.1098/rspa.1933.0193>.

J. J. Tao, Bruno Eckhardt, and X. M. Xiong. Extended localized structures and the onset of turbulence in channel flow. *Physical Review Fluids*, 3(1):011902, January 2018. doi: 10.1103/PhysRevFluids.3.011902. URL <https://link.aps.org/doi/10.1103/PhysRevFluids.3.011902>. Publisher: American Physical Society.

W. Tollmien. Über die Entstehung der Turbulenz. 1. Mitteilung. *Nachrichten von der Gesellschaft der Wissenschaften zu Göttingen, Mathematisch-Physikalische Klasse*, 1929:21–44, 1928. URL <http://eudml.org/doc/59276>.

Lloyd N. Trefethen. Pseudospectra of Linear Operators. *SIAM Review*, 39(3):383–406, January 1997. ISSN 0036-1445, 1095-7200. doi: 10.1137/S0036144595295284. URL <http://pubs.siam.org/doi/10.1137/S0036144595295284>.

Takahiro Tsukahara, Kaoru Iwamoto, Hiroshi Kawamura, and Tetsuaki Takeda. DNS of heat transfer in a transitional channel flow accompanied by a turbulent puff-like structure, September 2014a. URL <http://arxiv.org/abs/1406.0586>. arXiv:1406.0586 [physics].

Takahiro Tsukahara, Yasuo Kawaguchi, and Hiroshi Kawamura. An experimental study on turbulent-stripe structure in transitional channel flow, 2014b. URL <https://arxiv.org/abs/1406.1378>. Version Number: 2.

Takahiro Tsukahara, Yohji Seki, Hiroshi Kawamura, and Daisuke Tochio. DNS of turbulent channel flow at very low Reynolds numbers, September 2014c. URL <http://arxiv.org/abs/1406.0248>. arXiv:1406.0248 [physics].

Laurette S Tuckerman and Dwight Barkley. Patterns and dynamics in transitional plane Couette flow. *Physics of Fluids*, 23(4), 2011. ISSN 1070-6631. Publisher: AIP Publishing.

Laurette S. Tuckerman, Tobias Kreilos, Hecke Schröbsdorff, Tobias M. Schneider, and John F. Gibson. Turbulent-laminar patterns in plane Poiseuille flow. *Physics of Fluids*, 26(11):114103, November 2014. ISSN 1070-6631, 1089-7666. doi: 10.1063/1.4900874. URL <https://pubs.aip.org/pof/article/26/11/114103/315350/Turbulent-laminar-patterns-in-plane-Poiseuille>.

Geoffrey K. Vallis, Douglas J. Parker, and Steven M. Tobias. A simple system for moist convection: the Rainy–Bénard model. *Journal of Fluid Mechanics*, 862:162–199, March 2019. ISSN 0022-1120, 1469-7645. doi: 10.1017/jfm.2018.954. URL https://www.cambridge.org/core/product/identifier/S0022112018009540/type/journal_article.

D. Viswanath. Recurrent motions within plane Couette turbulence. *Journal of Fluid Mechanics*, 580:339–358, June 2007. ISSN 0022-1120, 1469-7645. doi: 10.1017/S0022112007005459. URL https://www.cambridge.org/core/product/identifier/S0022112007005459/type/journal_article.

Fabian Waleffe. Exact coherent structures in channel flow. *Journal of Fluid Mechanics*, 435:93–102, May 2001. ISSN 0022-1120, 1469-7645. doi: 10.1017/S0022112001004189. URL https://www.cambridge.org/core/product/identifier/S0022112001004189/type/journal_article.

Fabian Waleffe. Homotopy of exact coherent structures in plane shear flows. *Physics of Fluids*, 15(6):1517–1534, June 2003. ISSN 1070-6631, 1089-7666. doi: 10.1063/1.1566753. URL <https://pubs.aip.org/pof/article/15/6/1517/448391/Homotopy-of-exact-coherent-structures-in-plane>.

G. E. Willis and J. W. Deardorff. The oscillatory motions of Rayleigh convection. *Journal of Fluid Mechanics*, 44(04):661, December 1970. ISSN 0022-1120, 1469-7645. doi: 10.1017/S0022112070002070. URL http://www.journals.cambridge.org/abstract_S0022112070002070.

Xiangkai Xiao and Baofang Song. The growth mechanism of turbulent bands in channel flow at low Reynolds numbers. *Journal of Fluid Mechanics*, 883:R1, January 2020. ISSN 0022-1120, 1469-7645. doi: 10.1017/jfm.2019.899. URL https://www.cambridge.org/core/product/identifier/S0022112019008991/type/journal_article.

Shihe Xin, Xavier Nicolas, and Patrick Le Quéré. Stability analyses of Longitudinal Rolls of Poiseuille-Rayleigh-Bénard Flows in Air-Filled Channels of Finite Transversal Extension. *Numerical Heat Transfer, Part A: Applications*, 50(5):467–490, July 2006. ISSN 1040-7782, 1521-0634. doi: 10.1080/10407780600620079. URL <http://www.tandfonline.com/doi/abs/10.1080/10407780600620079>.

Xiangming Xiong, Jianjun Tao, Shiyi Chen, and Luca Brandt. Turbulent bands in plane-Poiseuille flow at moderate Reynolds numbers. *Physics of Fluids*, 27(4):041702, April 2015. ISSN 1070-6631, 1089-7666. doi: 10.1063/1.4917173. URL <https://pubs.aip.org/pof/article/27/4/041702/1019208/Turbulent-bands-in-plane-Poiseuille-flow-at>.